A Two - Temperature Statistical Model for Particle Production at High Energies

J. R. Wayland and T. Bowen

Department of Physics

University of Arizona

Tucson, Arizona

July 21, 1966

A Two - Temperature Statistical Model for Particle Production at High Energies*

J. R. Wayland and T. Bowen

Summary

With the assumption of two characteristic temperatures, one associated with the transverse momentum distribution, the other with the longitudinal, the differential cross section, $\frac{d^2N}{dp\,d\Omega}$, is calculated from the relativistic quantum statistical mechanical number density. Good agreement with experimental data for pions, kaons, and antiprotons is obtained by the fitting of T_0, the transverse temperature, T, the longitudinal temperature, and V_0, the interaction volume. The model is related to a simple physical interpretation.

---

*This work was partly supported by NASA Grant NGR-03-002-071.

A Two - Temperature Statistical Model for

Particle Production at High Energies

J. R. Wayland and T. Bowen

Department of Physics, University of Arizona, Tucson, Arizona

1. - Introduction.

There have been many attempts to find expressions for the spectra of particles produced in proton-proton and proton-nuclei collisions ([1]). All but one has had rather limited success in explaining known spectra of produced particles. The most successful attempt assumes longitudinal and transverse particle momentum distributions suggested by experimental results ([2]). Starting with a basic equation from quantum statistical mechanics, we will derive expressions for the momentum distributions. These distributions will be used to obtain an expression for $d^3N/dpd\Omega$.

We will assume that there are two characteristic temperatures: one associated with the transverse distribution, the other with the longitudinal. This is suggested by the remarkable independence of the transverse particle.

([1]) M. Kretzschmar, Ann. Rev. Nucl. Sci., 11, 1 (1961).

([2]) G. Cocconi, D. H. Perkins, L. J. Koester, Study #28 of Berkeley High Energy Physics Study, UCRL-10022 (unpublished).

momentum distribution from the energy of the incident particle. One can consider this as a decoupling of the temperatures which could occur because of the more rapid dispersal of energy associated with the longitudinal motion. Another suggestion comes from the assumed rotational ellipsoid form of the interaction volume. The longitudinal dimension is dependent upon the energy of the incoming particle under a Lorentz transformation, but the transverse dimension is independent of energy.

2. - Derivation of Differential Cross Section.

One can find from a quantum statistical mechanical analysis that the average occupation numbers for particles produced in a high energy interaction can be written [3]

$$(1) \qquad \bar{\nu}_{\alpha k} = \frac{1}{e^{\sqrt{p_\alpha^2 + m_k^2}/T} \mp 1}$$

where, as is usual, the negative sign is for bosons and the positive sign is for fermions. However, equation (1) is not relativistically invariant. Relativistic invariance requires the exponent to be written in an invariant form. The exponent can be written as $\beta k_\nu U^\nu$, where k_ν is the four momenta and U^ν is the four-velocity [4]. ($\beta = 1/T$). Only in the C.M. system will $\beta k_\nu U^\nu = \sqrt{p_\alpha^2 + m_k^2}\,/T$.

The distribution of longitudinal particle momentum, $p_\parallel$, for a given

(3) R. Hagedorn, Nuovo Cimento Supp. III, No. 2, 147 (1965).

(4) K. Just (private communications);

J. L. Synge, The Relativistic Gas, Interscience Publ., New York (1957).

mass in momentum space is found by integrating (1) over $dp_\perp$. (We have changed to the variables $p_\parallel$ and $p_\perp$, the longitudinal and transverse momentum respectively.) We define $\mu_1^2 = p_\parallel + m_k^2$. Noting that $K_{1/2}(x) = \sqrt{1/2x}\; e^{-x}$ (modified Bessel Functions of the second type), and $1/(e^x - 1) = \sum_{k=1}^{\infty} e^{-kx}$ we can write for bosons [5]

$$(2) \qquad \omega_\parallel(p_\parallel)dp_\parallel = A \sum_{k=1}^{\infty} \left(\frac{2k}{\pi T}\right)^{1/2} dp_\parallel \int_0^\infty p_\perp (p_\perp^2 + \mu_1^2)^{1/4} K_{1/2}\left[\frac{k(p_\perp^2 + \mu_1^2)^{1/2}}{T}\right] dp_\perp ,$$

$$= \sum_{k=1}^{\infty} A\left(\frac{2T}{k\pi}\right)^{1/2} dp_\parallel \; \mu_1^{3/2} K_{3/2}(k\mu_1/T) ,$$

where $A = 2\pi V_0/h^3$ and V_0 is the interaction volume. Upon normalization, this becomes

$$(3) \qquad \omega_\parallel^{(N)}(p_\parallel)dp_\parallel = \sqrt{\frac{2}{\pi T}} \; \frac{\mu_1^{3/2}}{m^2 c^3} \; \frac{\sum_{k=1}^{\infty} K_{3/2}\left(\frac{k\mu_1}{T}\right)/\sqrt{k}}{\sum_{k=1}^{\infty} \frac{K_2(kmc^2/T)}{k}} \; dp_\parallel .$$

We have used $c = \hbar = 1$ and then inserted c and $\hbar$ in the final expression. We can use the expression for $K_{3/2}(k\mu_1/T)$ to find

$$(4) \qquad \omega_\parallel^{(N)}(p_\parallel)dp_\parallel = \frac{T}{m^2 c^3} \; \frac{\sum_{k=1}^{\infty} \frac{e^{-k\mu_1/T}}{k^{3/2}} \left(1 + \frac{k\mu_1}{T}\right)}{\sum_{k=1}^{\infty} \frac{K_2(km/T)}{k}} \; dp_\parallel .$$

Likewise, to obtain the transverse momentum distribution we integrate over $dp_\parallel$:

---

(5) We can also write $1/(e^x + 1) = \sum_{k=1}^{\infty} (-1)^{k+1} e^{-kx}$. Thus, for fermions, the results should contain a $(-1)^{k+1}$ in each series.

$$(5)\qquad \omega_\perp(p_\perp)dp_\perp = A \sum_{k=1}^{\infty} p_\perp \left(\frac{2k}{\pi T_0}\right)^{1/2} dp_\perp \int_0^\infty (p_\parallel^{\,2} + \mu_2)^{1/4} K_{1/2}\left[\frac{k(p_\parallel^{\,2} + \mu_2^{\,2})^{1/2}}{T_0}\right] dp_\parallel$$

$$= \sum_{k=1}^{\infty} A\, p_\perp\, \mu_2\, K_1(k\mu_2/T_0)\, dp_\perp\ ,$$

where $\mu_2^{\,2} = p_\perp^{\,2} + m^2$. When we normalize this, we find [6]

$$(6)\qquad \omega_\perp^{(N)}(p_\perp)dp_\perp = \frac{p_\perp \mu_2}{T_0 m^2 c^2} \frac{\sum_{k=1}^{\infty} K_1(k\mu_2/T_0)}{\sum_{k=1}^{\infty} \frac{K_2(kmc^2/T_0)}{k}} dp_\perp\ .$$

By not equating T and T_0 we have introduced two temperatures and thus assumed that $p_\perp$ and $p_\parallel$ are approximately independent (some justification for this can be found in Appendix A). One would also expect this from an inspection of the shape of the interaction volume. The interaction volume is a flat disk. One could think of the transverse displacements as caused by the "transverse temperature" and the "thickness" of the disk as associated with the "longitudinal temperature".

---

[6] K. Imaeda and J. Avidan, (Nuovo Cimento 32, 1497 (1964)), have also obtained Equation 6 for bosons, which they refer to as Planck's distribution. They show that this distribution gives a satisfactory fit to data from cosmic ray jets and that a distribution of the form $\omega_\perp(p_\perp)dp_\perp = 2\,\alpha\, p_\perp \exp(-\alpha\, p_\perp^{\,2})dp_\perp$ gives a much poorer fit. H. H. Aly, M. F. Kaplon and M. L. Shen, (Nuovo Cimento 32, 905 (1964)); and E. M. Friedländer (Nuovo Cimento 41, 417 (1966)), have made the erroneous assertion that the latter form is necessarily implied by the assumption of axial symmetry. Aly, et al., reached this mistaken conclusion by imposing too strong a condition on the form of the distribution function: namely, that $\omega(p_\perp) = f(p_x) \cdot f(p_y)$. This is only true if p_x and p_y are statistically independent, which is not necessary for axial symmetry.

The probability of obtaining a particle of mass m and momentum $p_\parallel$ and $p_\perp$ is given by

$$(7) \qquad P(p_\parallel, p_\perp)\, dp_\parallel\, dp_\perp = N(T)\, \omega_\parallel^{(N)}(p_\parallel)\, \omega_\perp^{(N)}(p_\perp)\, dp_\perp\, dp_\parallel \;.$$

Here N(T) is the number of particles obtained from integrating equation (1) over $dp_\perp\, dp_\parallel$. We have assumed that N is determined by the longitudinal temperature. This gives

$$(8) \qquad N = \frac{V_0 mc^2 T}{h^3} \sum_{k=1}^{\infty} \frac{K_2(kmc^2/T)}{k} \;.$$

If $d\Omega$ is the differential solid angle the transformation from $dp d\Omega$ to $dp_\parallel dp_\perp$ is

$$(9) \qquad \frac{dp_\parallel dp_\perp}{dp d\Omega} = \frac{2p^2}{p_\perp} \;,$$

where p is the total momentum of the particle. The flux is found with the aid of (5), (6), (7), (8), and (9):

$$(10) \qquad \frac{d^2N}{dp^* d\Omega^*} = \frac{2V_0T^4}{T_0 m^2 c^4 h^3} \left(\frac{p}{T}\right)^2 \mu_2 \frac{\left(\sum_{k=1}^{\infty} K_1(ku_2/T_0)\right)\left(\sum_{k=1}^{\infty} e^{-\frac{k\mu_1}{T}} \left(1 + \frac{k\mu_1}{T}\right)/k^{3/2}\right)}{\sum_{k=1}^{\infty} \frac{K_2(kmc^2/T_0)}{k}}$$

The average values of $p_\parallel$ and $p_\perp$ are found in Appendix B.

We have calculated the differential cross-section $\frac{\partial^2 N(p^*, \theta^*)}{\partial p^* \partial\Omega^*}$ in the C.M. and it is related to the laboratory differential cross-section by

$$(11) \qquad \frac{\partial^2 N(p, \theta)}{\partial p d\Omega} = \frac{\partial^2 N(p^*, \theta^*)}{\partial p^* \partial\Omega^*} \frac{E^* p^2}{E\, p^{*2}} \;.$$

We will fit equation (10) to spectra in the C.M. system (at angles in the forward and backward cones) and use the above transformation to obtain the spectra in the laboratory system. The interaction volume, V_0, will act as a free constant to determine the normalization to experimental data.

3.- Comparison with Experiment.

A. The Pion Spectra.

From cosmic ray and machine-produced particles we know that for pions $0.2 \leq \langle p_\perp \rangle \leq 0.6$ Bev/c as $6 \leq E_0 \leq 10^5$ Bev ([7]). When $\langle p_\perp \rangle \approx 0.4$ Bev/c we find with the aid of (B.3) that $T_0 \approx 0.16$ Bev. For comparing the above results with experimental data in the 10 to 30 Bev range, we will assume that $\langle p_\perp \rangle$ is constant, since experimental data indicates that, at most, $\langle p_\perp \rangle \sim \ln E_0$ ([7]). When one makes a best fit to the data from the AGS, the parameter $T = 0.38$ Bev for normalization to the 4.75° and 20° data ([8]) (corresponding to forward and backward cones in the C.M.).

To make the transformation from one incident particle energy to another, we note that

$$(12) \qquad n_s \langle E_s \rangle = K_s E_0 \quad ,$$

where K_s is the fraction of the total energy content possessed by the secondaries of type s, and $\langle E_s \rangle$ is the average energy of the secondaries. If one uses equation (1) to calculate the average energy it is found that $\langle E \rangle \propto T^4$ with the condition $m/T \to 0$. Even with m/T of the order of one this is a fair

---

([7]) V. S. Barashenkov, V. M. Mal'tser and I. Patera, JINR-P-1577 (unpublished).

([8]) Baker, et al., Phys. Rev. Letters 7, 101 (1961).

approximation. Thus we can assume that $n_s \propto E_o^{1/4}$. D. H. Perkins gives n_s = number of charged secondaries $= 1.8\, E_o^{1/4}$ and the ratio of charged pions to all charged secondaries as 0.82 ± 0.05 (9). Thus $n_{\pi^\pm} = 1.5\, E_o^{1/4}$. At $E_o = 30$ Bev, $n_{\pi^\pm} = 3.5$. We are interested in either π^+ or π^-, so if $n_{\pi^+} = n_{\pi^-}$ we have $n_\pi \approx n_{\pi^+} \approx n_{\pi^-} \approx 1.7$. Using equation (B.2) we can find $\langle E_s^* \rangle$ as a function of T. From the value of $\langle E_s^* \rangle$ we find $\langle E_s \rangle$. For

$$K_\pi = \frac{n_\pi \langle E_\pi \rangle}{E_o} \tag{13}$$

we find $K_\pi = .26$. The results of fitting equation (10) with the aid of (11) to the pion spectra are shown in Figures 1, 2, 3, 4, 5, and 6 for various angles and incident energies (10). Because of the approximations of the statistical model used, the fit is not expected to be good for < 15 Bev.

We can take the interaction volume in the above analysis to be an ellipsoid with two of the axes equal to the Compton wavelength corresponding to the temperature T_0 and one to the temperature T.

$$V_0 = \frac{4\pi}{3} \left(\frac{\alpha\hbar}{T_0} c\right)^2 \left(\frac{\alpha\hbar}{T} c\right) . \tag{14}$$

One would expect α to be of the order of one. For a reasonable fit to the pion data, we find $T = 0.38$ Bev, and $\alpha = 0.56$.

B. The Kaon Spectra.

When one applies this approach to the positive kaon spectra from the AGS (8), the best results are obtained for $T_0 = 0.160$ Bev and $T = 0.38$ Bev.

---

(9) D. H. Perkins, Study #10, 11, of Berkeley High Energy Physics Study, UCRL-10022 (unpublished).

(10) D. Dekhers, et al., Phys. Rev. 137, B962 (1965).

This is shown in Fig. 6. Because of the difference in the production channels open to negative kaons we have fitted its spectra with $T_0 \approx 0.160$ Bev and $T = 0.30$ Bev. This is also shown in Fig. 6 [11]. In fitting the kaon data we have used an average for $\langle p_\perp \rangle = 0.46$ Bev/c [7] and to estimate the inelasticity coefficient we have taken $n_{K^-}/n_{\pi^-} \approx 0.04$.

C. The Antiproton Spectra.

We can use the same type of analysis to fit the antiproton spectra. If we take $T_0 = 0.160$ and $T = 0.160$ Bev, the results of applying equation (10) with the aid of equation (11) are shown in Figs. 7 and 8. Again we have assumed that $n_{\bar{p}} \propto E_0^{1/4}$ and have taken $n_{\bar{p}}/n_{\pi^-} \approx 10^{-2}$ (in order to find the inelasticity coefficient K).

D. Results.

With adjustment of three parameters it is possible to obtain good agreement with experimental data over a large range of incident energy, lab angle, and secondary particle momentum. The method works equally well for different types of particles. The results for the various parameters are given in Table I. One notes that: (a) the transverse temperature, T_0, is the same for all particles; (b) the longitudinal temperature, T, is the same for pions and K^+, decreases for K^-, and further decreases until it is equal to the transverse temperature for $\bar{p}$ [12].

---

[11] It is also possible to fit the CERN data with an expression of the type of equation (10).

[12] Imaeda and Avidan obtain a value for T_0 of 0.122 Bev, somewhat lower than our value. However, they obtained this value from secondary particles produced in cosmic-ray jets.

One can drop the summation from the above equations, keeping only the k=1 term, without changing the results significantly. Then we can write equation (10) as

$$(15) \qquad \frac{d^2N}{dp^* d\Omega^*} = \frac{2V_0T^4}{T_0h^3m^2c^4K_2(mc^2/T_0)} \left(\frac{p}{T}\right)^2 \mu_2K_1(\mu_2/T_0)\ e^{-\mu_1/T}\left(1+\frac{\mu_1}{T}\right) \ .$$

It is interesting to note that the interaction volume, V_0, for pions is approximately ten times greater than for kaons and 100 times greater than the antiproton volume. One also notices the following: (a) the fit is not good in the low (1 to 3 Bev/c) secondary momentum range for low production angles for complex nuclear targets; (b) the 0° spectra changes markedly from that of angles greater than 0°; (c) in the pion spectra there is a large difference between the π^+ and π^-. When one examines the number of particles in the C.M. system at high momentum in the backward direction from heavy target nuclei it is found that there are more particles produced than predicted by this model. This is probably due to the nucleon-nucleus interaction involving more than one nucleon in the target nucleus. This would account for (a). However, (b) and (c) cannot be accounted for by this analysis.

4. - Discussion.

An inspection of the results of fitting equation (10) to the spectra for different particles indicates that there is rather good agreement with experimental data for: (a) $E_0 > 15$ Bev; (b) secondary momentum greater than about 3 Bev/c for small angles; (c) angles $\gtrsim 20°$. Also, the inelasticity coefficient, K, is within the measured range of experimental values (but, perhaps, a little large).

Basically we have assumed that the production process occurs by creation of a fireball that in turn "boils off" the secondary particles. The momentum distribution of particles in the fireball is a combination of two approximately independent distributions characterized by two temperatures. T_0 determines the transverse distribution and T the longitudinal distribution and number of particles produced via the quantum mechanical number density. The longitudinal and transverse modes appear to be only weakly coupled during the expansion of the fireball. Antiprotons seem to be boiled off at a stage of the interaction process when the transverse temperature, T_0, and the longitudinal temperature, T, are approximately the same; the pions and kaons, at unequal temperatures. Because of the flat disk shape of the interaction volume, the transverse modes remain coupled among groups of particles longer than the longitudinal modes while the particles are moving apart toward eventual freedom. As a result, the transverse momentum distribution of a boiled-off particle may be characterised by a lower temperature than its longitudinal momentum distribution.

TABLE I

Particle	T_0 (Bev)	T(Bev)	K	α
π^+ or π^-	0.16	0.38	0.26	0.56
K^+	0.16	0.38	0.032	0.75
K^-	0.16	0.30	0.0109	0.824
$\bar{p}$	0.16	0.16	0.0043	0.231

* * * *

The authors wish to thank Dr. K. Just for a very helpful discussion. Also, we would like to thank Dr. R. Hagedorn for sending us copies of his paper before publication.

Appendix A - The Correlation Coefficient.

To check the possibility of expressing a given distribution of known form as the product of two new functions, one should compute the correlation coefficient. In our case,

$$P(p) \overset{?}{=} \omega_{\parallel}^{(n)}(p_{\parallel})\, \omega_{\perp}^{(n)}(p_{\perp}) \tag{A.1}$$

can be checked by computing the correlation coefficient, ρ

$$\rho = \frac{\langle (p_{\perp} - \langle p_{\perp}\rangle)\,(p_{\parallel} - \langle p_{\parallel}\rangle)\rangle}{\langle (p_{\parallel} - \langle p_{\parallel}\rangle)^2\rangle^{1/2}\,\langle (p_{\perp} - \langle p_{\perp}\rangle)^2\rangle^{1/2}} \;. \tag{A.2}$$

We find that

$$\rho = \frac{\left[K_3(m/T) - \dfrac{K_{5/2}^{\,2}(m/T)}{K_2(m/T)}\right]}{\left[K_3(m/T) - \dfrac{2K_{5/2}^{\,2}(m/T)}{\pi K_2(m/T)}\right]^{1/2}\left[4\,K_3(m/T) - \dfrac{\pi K_{5/2}^{\,2}(m/T)}{2\,K_2(m/T)}\right]^{1/2}} \tag{A.3}$$

As we go to higher energies $m/T \to 0$ and $\rho \to 0.109$. (For pions $\rho \to 0.103$ at $E_0 = 30$ Bev.) ρ decreases slowly for increasing m/T. We can assume that (A.1) is a reasonable approximation. We also remark that p_x and p_y are not strictly statistically independent, a requirement which several authors have mistakenly imposed ([6]).

Appendix B - Derivation of $\langle p_\perp \rangle$ and $\langle p_\parallel \rangle$

For the normalization of $\omega_\parallel$ and $\omega_\perp$ distributions we note that for $\omega_\parallel$

(B.1a) $$1 = \Omega\, A \left(\frac{2}{\pi T}\right)^{1/2} T \int_0^\infty (p_\parallel^{\,2} + m^2)^{3/4}\, K_{3/2} \left[\frac{(p_\parallel^{\,2} + m^2)^{1/2}}{T}\right] dp_\parallel$$

$$= \Omega\, A\, m^2\, T\, K_2\, (m/T),$$

and for $\omega_\perp$

(B.1b) $$1 = \Omega_0\, A \int_0^\infty p_\perp (p_\perp^{\,2} + m^2)^{1/2}\, K_1 \left[\frac{(p_\perp^{\,2} + m^2)^{1/2}}{T_0}\right] dp_\perp$$

$$= \Omega_0\, A\, m^2\, T_0\, K_2\, (m/T_0) \quad .$$

Now

(B.2) $$\langle p_\parallel \rangle = \Omega\, A \int_0^\infty p_\perp\, dp_\perp \int_0^\infty p_\parallel\, dp_\parallel\, e^{-\frac{(p_\parallel^{\,2} + \mu_2^{\,2})^{1/2}}{T}}$$

$$= \left(\frac{2mT}{\pi}\right)^{1/2} \frac{K_{5/2}\, (m/T)}{K_2\, (m/T)} \quad ,$$

and

(B.3) $$\langle p_\perp \rangle = \Omega_0\, A \int_0^\infty p_\perp^{\,2}\, dp_\perp \int_0^\infty dp_\parallel\, e^{-\frac{(p_\parallel^{\,2} + \mu_2^{\,2})^{1/2}}{T_0}}$$

$$= \left(\frac{\pi m T_0}{2}\right)^{1/2} \frac{K_{5/2}\, (m/T_0)}{K_2\, (m/T_0)} \quad .$$

The universal function $K_{5/2}(x)/((x)^{1/2}\, K_2(x))$ is shown in Fig. 9.

Figure Captions

Fig. 1. Momentum spectra of pions at 4.75° and 9°, observed at an incident energy of 10 Bev. [8]. (50% target efficiency).

Fig. 2. Momentum spectra of pions at 0° and 5.7°, observed at an incident energy of 18.8 Bev/c. [10].

Fig. 3. Momentum spectra of pions at 4.75° and 9°, observed at an incident energy of 20 Bev. [8]. (50% target efficiency).

Fig. 4. Momentum spectra of pions at 0° and 5.7°, observed at an incident energy of 23.1 Bev/c. [10].

Fig. 5. Momentum spectra of pions at 4.75°, 9°, 13°, 20°, and 45°, observed at an incident energy of 30 Bev. [8]. (50% target efficiency).

Fig. 6. Momentum spectra of kaons at 4.75°, 9°, 13°, and 20°, observed at an incident energy of 30 Bev. [8]. (50% target efficiency).

Fig. 7. Momentum spectra of antiprotons at 4.75°, 9°, and 13°, observed at an incident energy of 30 Bev. [8].

Fig. 8. Momentum spectra of antiprotons at 0° and 5.7°, observed at an incident energy of 23.1 Bev/c. [10].

Fig. 9. The function $\dfrac{K_{5/2}(x)}{\sqrt{x}\,K_2(x)}$ given as a function of $x = m/T$.

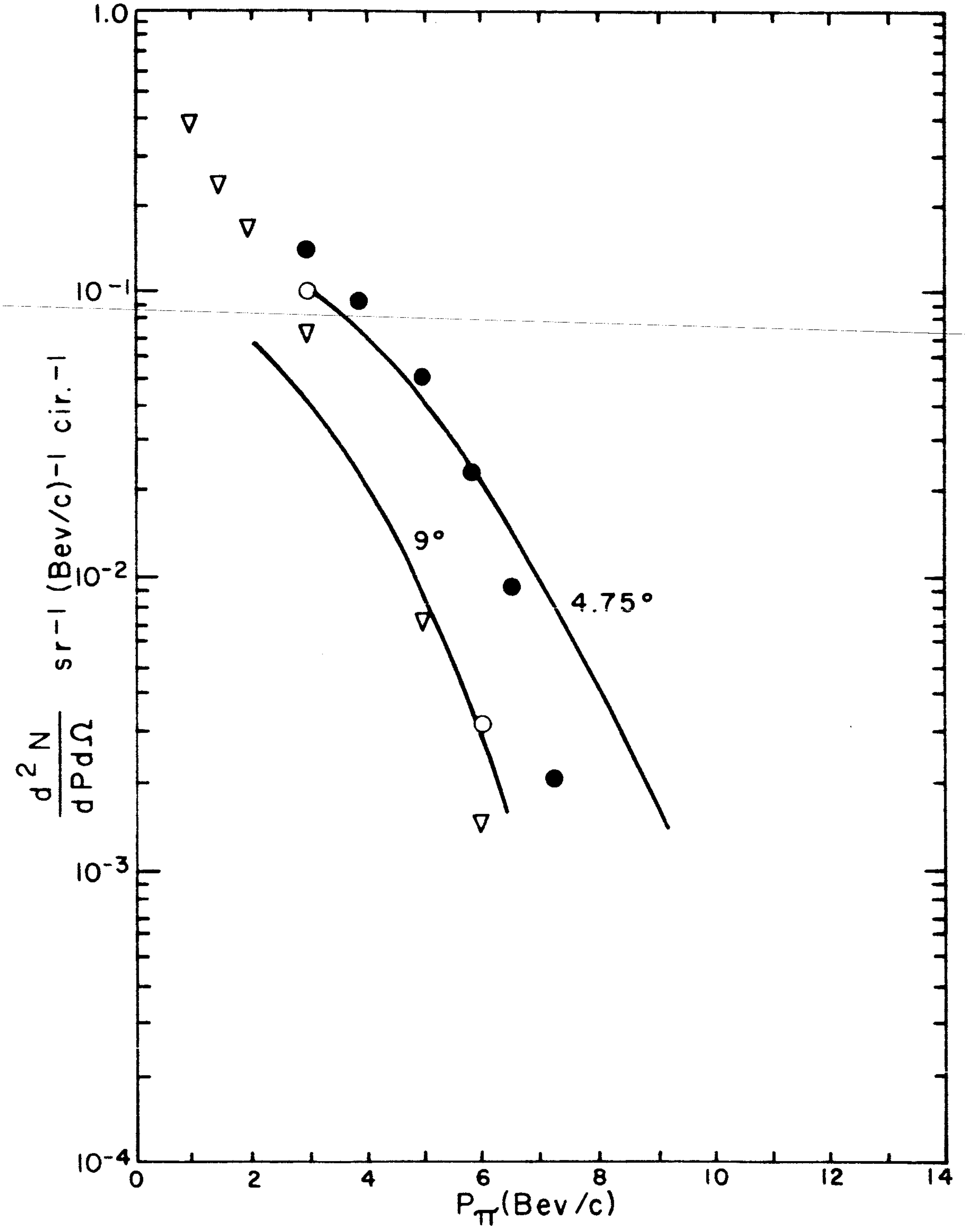

1.0
10^{-1}
10^{-2}
10^{-3}
10^{-4}
0
2
4
6
8
10
12
14
$\frac{d^2N}{dPd\Omega}$ sr^{-1} $(Bev/c)^{-1}$ $cir.^{-1}$
9°
4.75°
P_{π}(Bev/c)

FIGURE 1

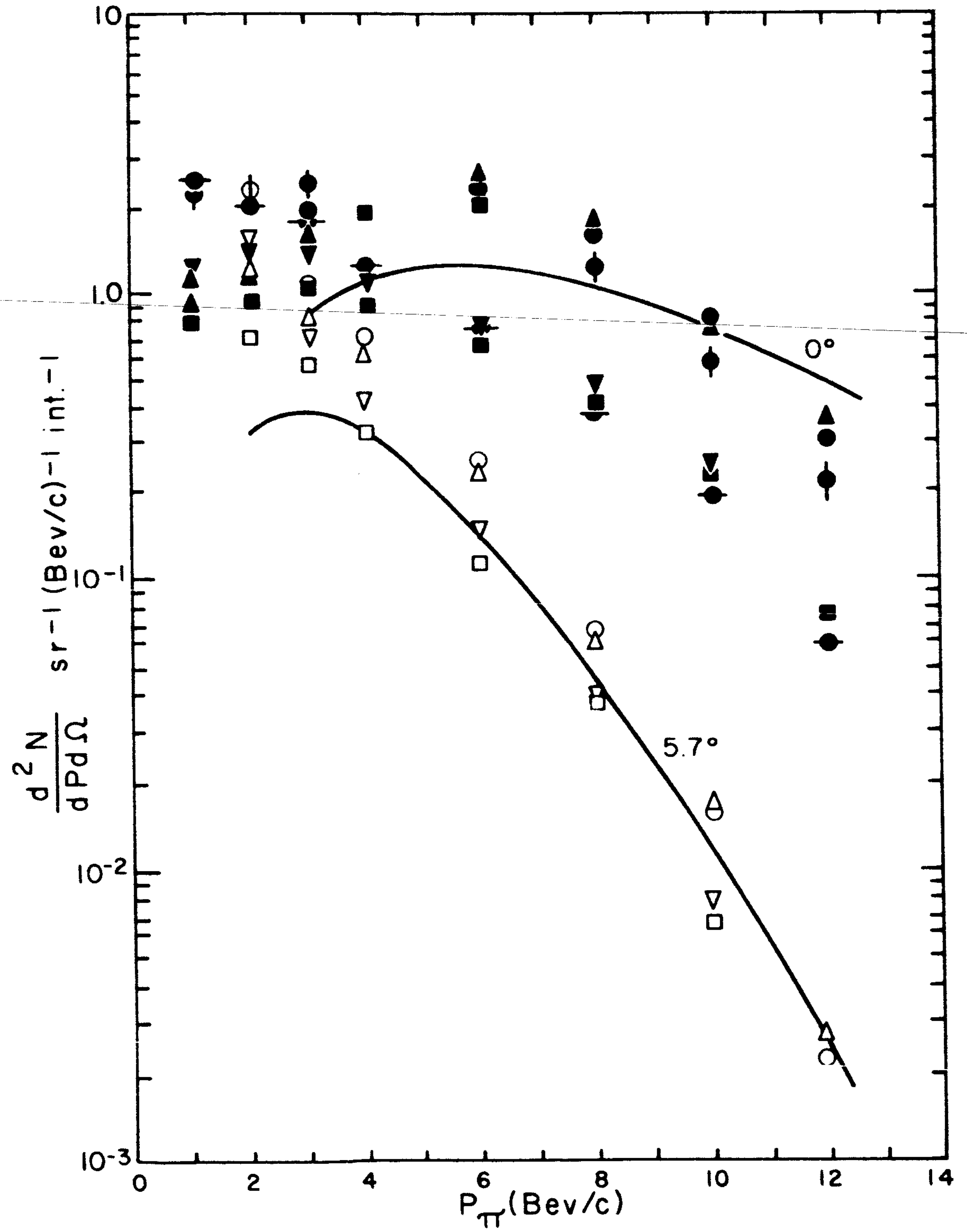

10
1.0
10^{-1}
10^{-2}
10^{-3}
0 2 4 6 8 10 12 14
$\frac{d^2N}{dPd\Omega}$ sr−1 (Bev/c)−1 int.−1
P_π (Bev/c)
0°
5.7°

FIGURE 2

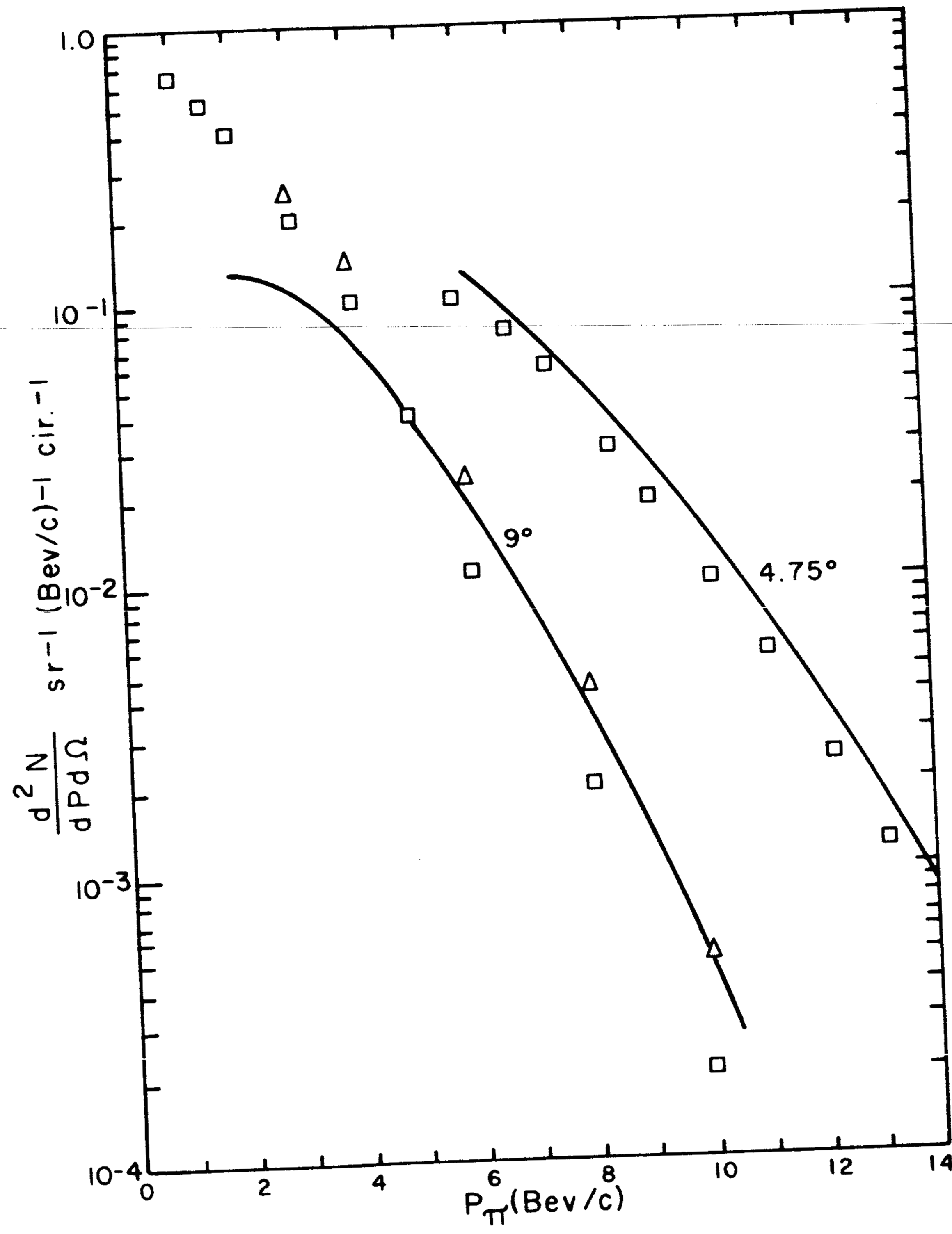
1.0
10⁻¹
10⁻²
10⁻³
10-4
0
2
4
6
8
10
12
14
$\frac{d^2N}{dPd\Omega}$ sr⁻¹ (Bev/c)⁻¹ cir.⁻¹
P_π(Bev/c)
9°
4.75°

FIGURE 3

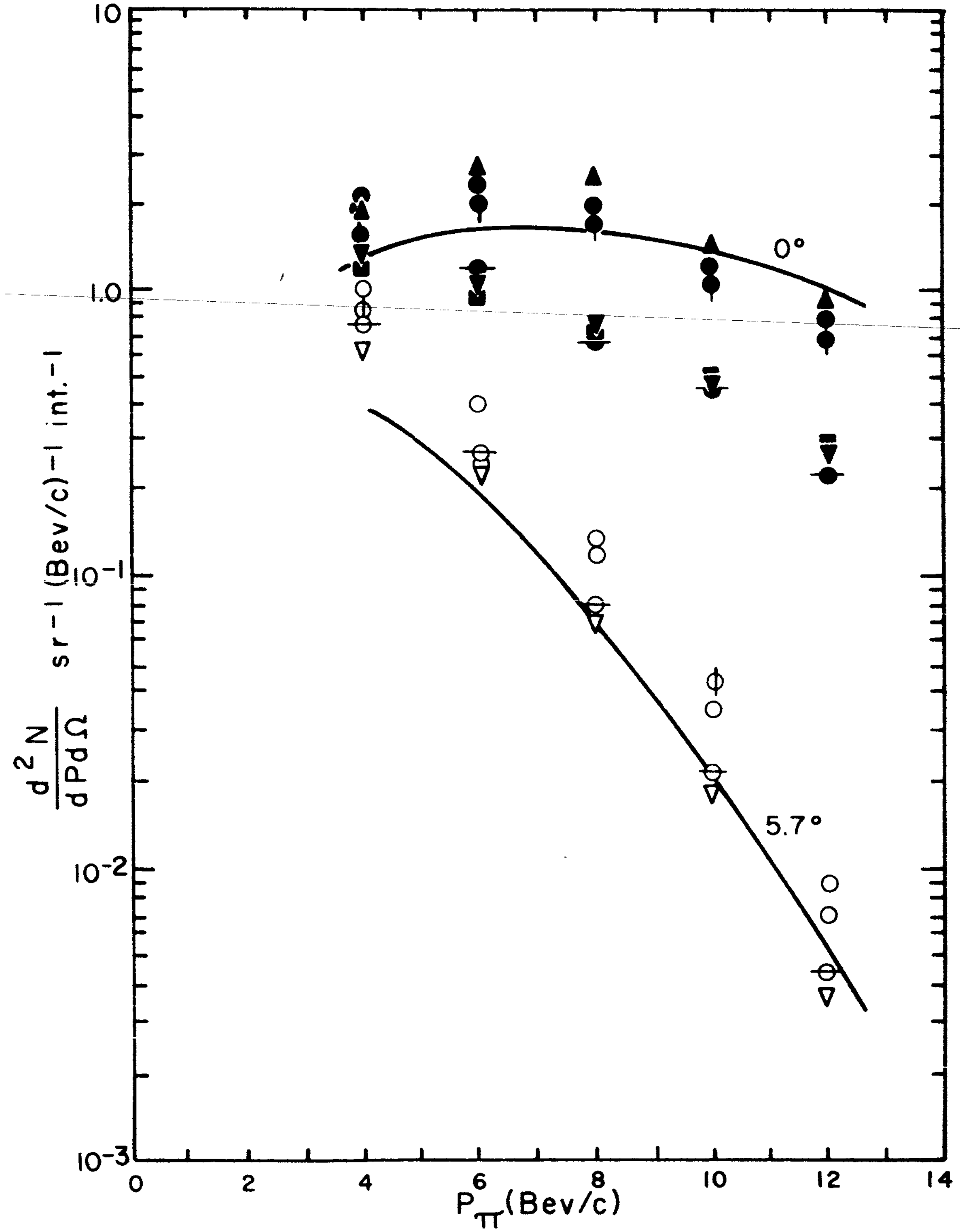

10
1.0
10^{-1}
10^{-2}
10^{-3}
$\frac{d^2N}{dPd\Omega}$ sr^{-1} (Bev/c)$^{-1}$ int.$^{-1}$
0°
5.7°
0
2
4
6
8
10
12
14
P_π(Bev/c)

FIGURE 4

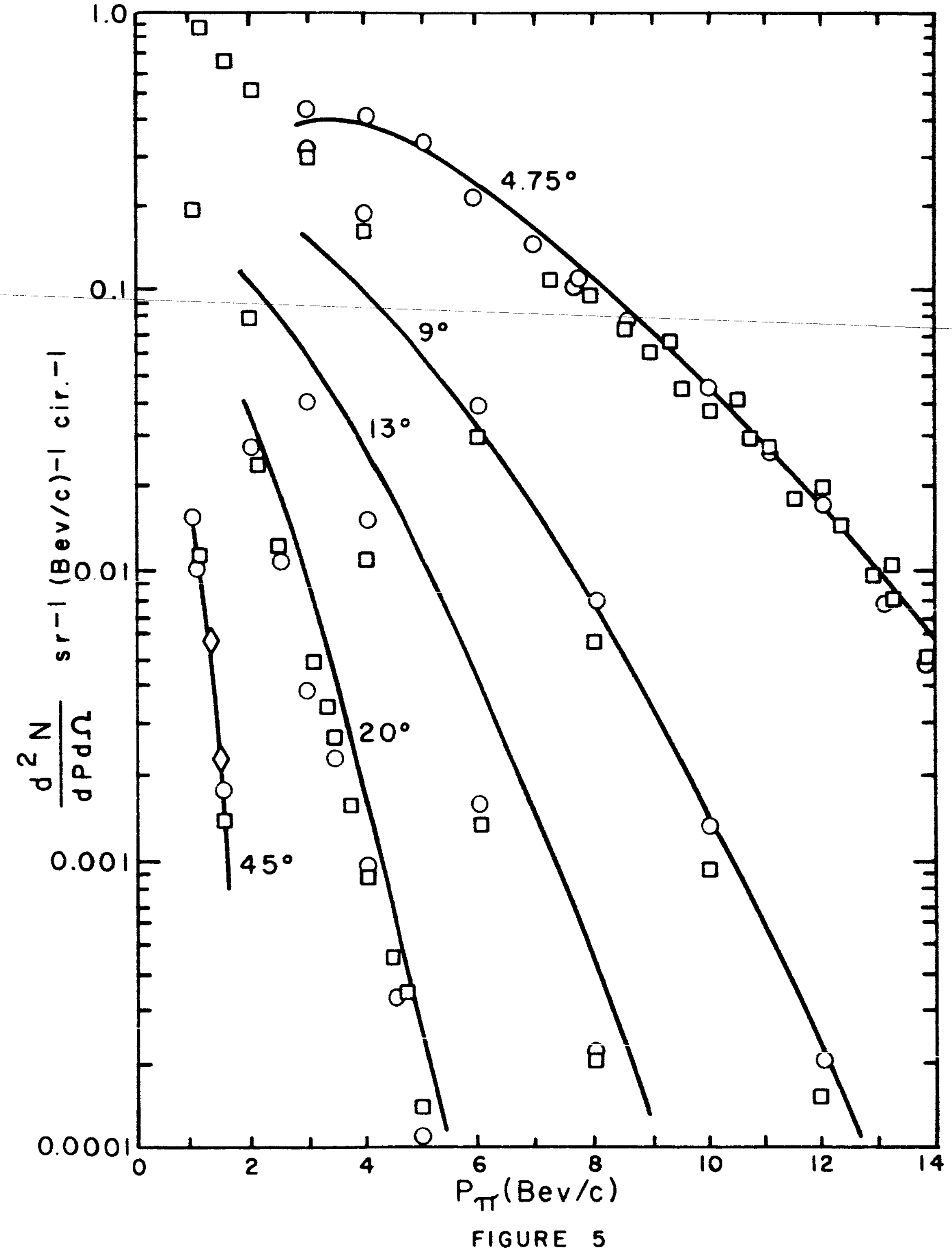

1.0
0.1
0.01
0.001
0.0001
0
2
4
6
8
10
12
14
$\frac{d^2N}{dPd\Omega}$ sr−1 (Bev/c)−1 cir.−1
P_π (Bev/c)
4.75°
9°
13°
20°
45°

FIGURE 5

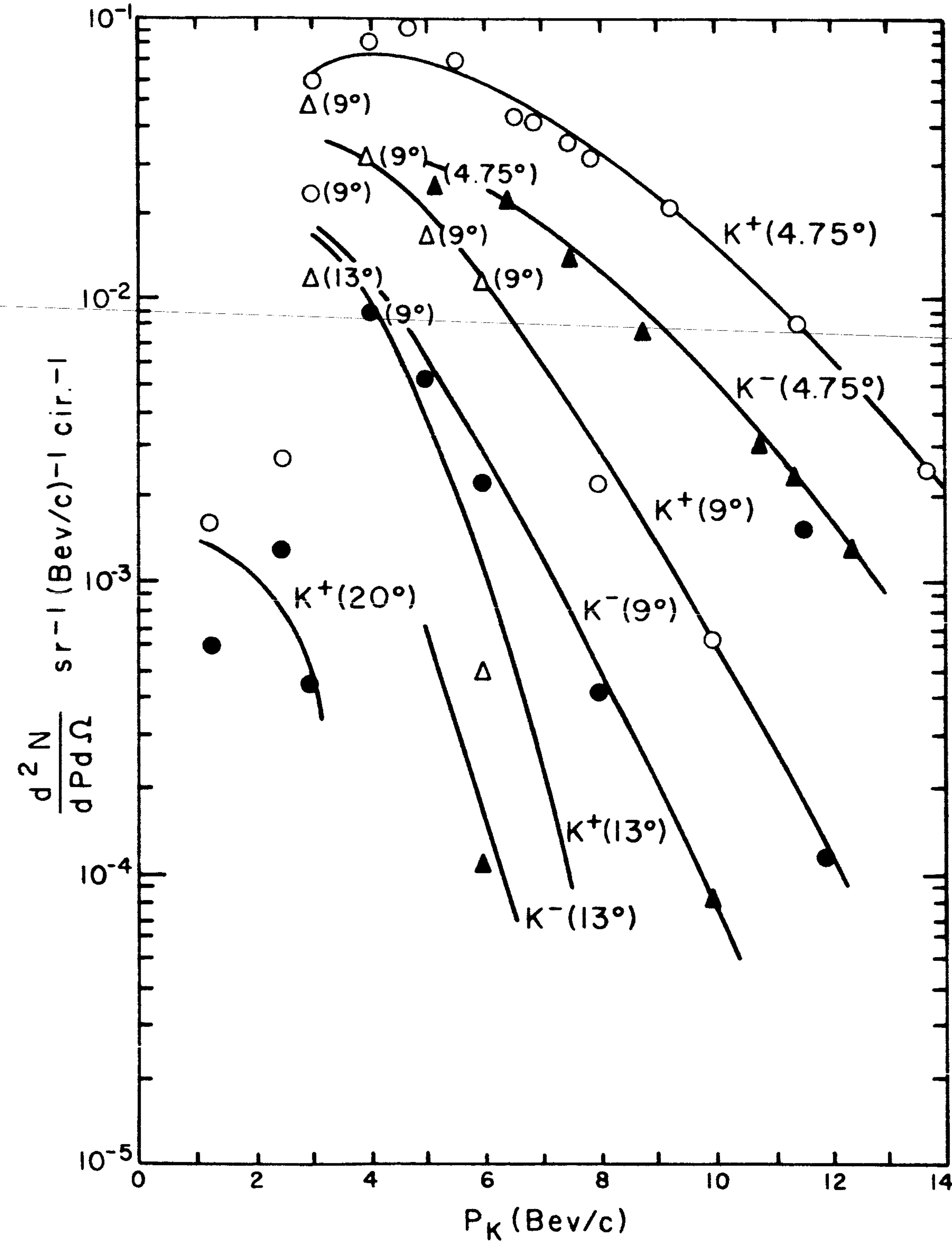

10^{-1}
10^{-2}
10^{-3}
10^{-4}
10^{-5}
0
2
4
6
8
10
12
14
$\frac{d^2N}{dPd\Omega}$ sr^{-1} (Bev/c)$^{-1}$ cir.$^{-1}$
P_K (Bev/c)
Δ(9°)
Δ(9°)
▲(4.75°)
○(9°)
Δ(9°)
Δ(9°)
Δ(13°)
●(9°)
K^+(4.75°)
K^-(4.75°)
K^+(9°)
K^+(20°)
K^-(9°)
Δ
K^+(13°)
K^-(13°)

FIGURE 6

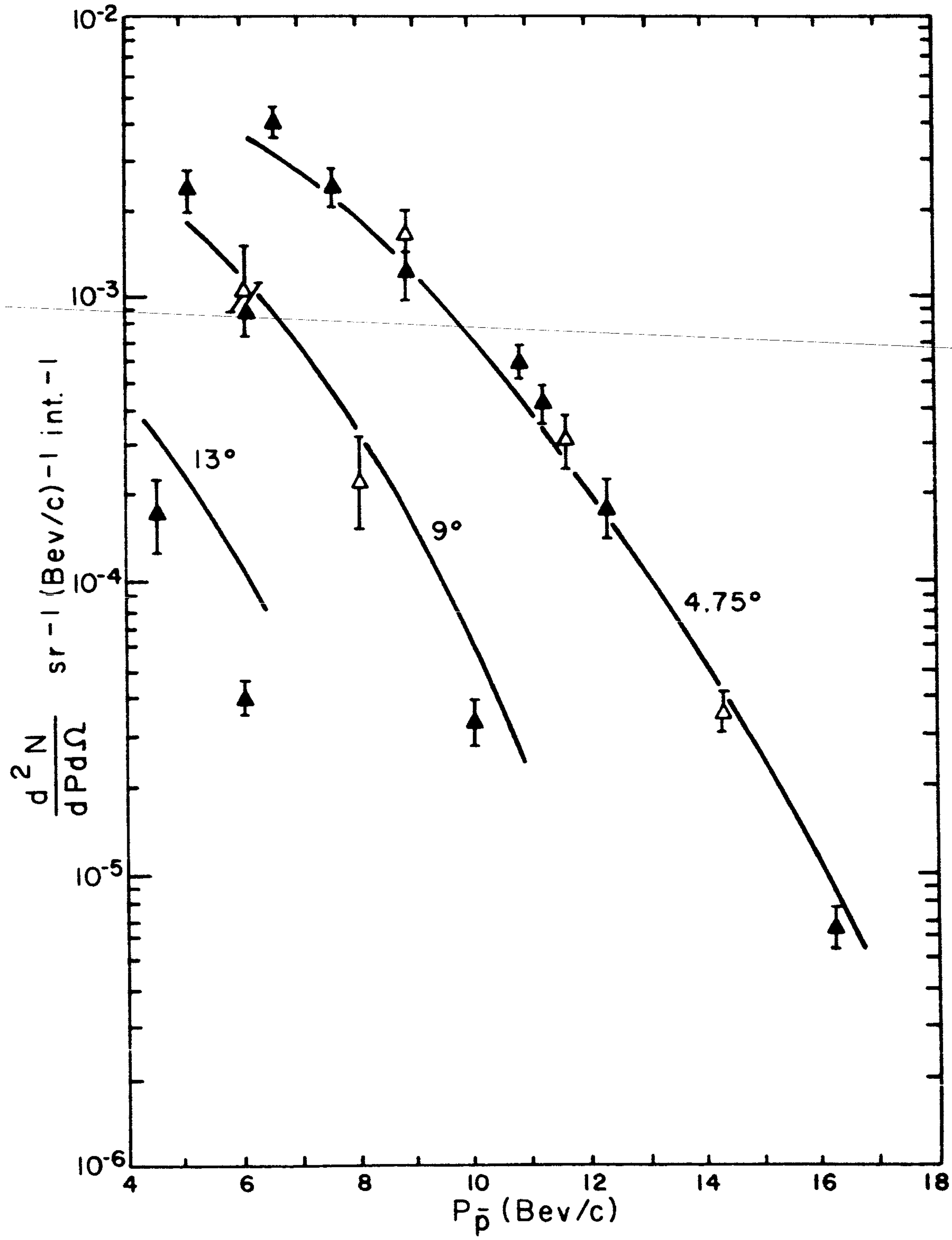

10^{-2}
10^{-3}
10^{-4}
10^{-5}
10^{-6}
$\frac{d^2N}{dPd\Omega}$ sr^{-1} (Bev/c)$^{-1}$ int.$^{-1}$
13°
9°
4.75°
4
6
8
10
12
14
16
18
$P_{\bar{p}}$ (Bev/c)

FIGURE 7

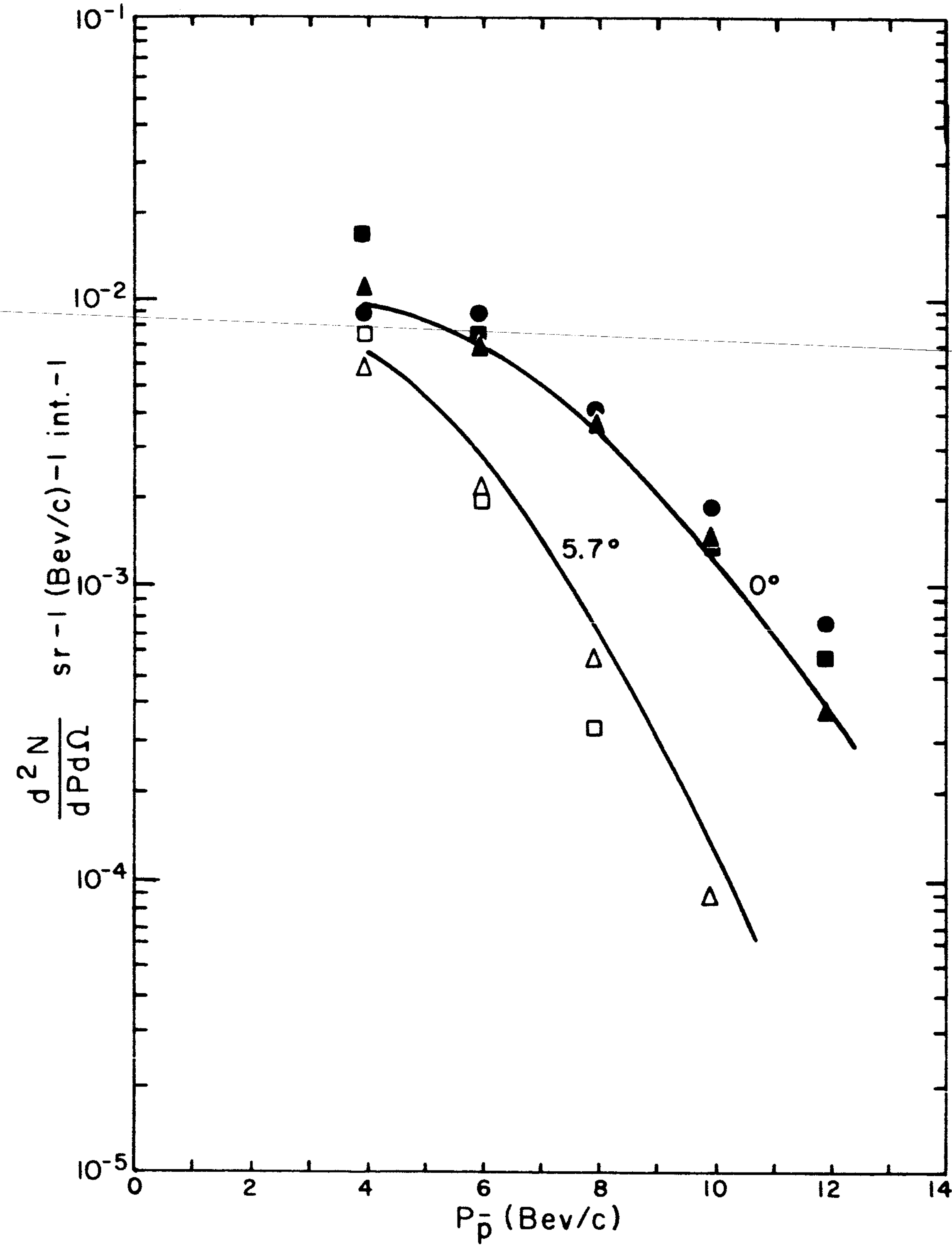
10^{-1}
10^{-2}
10^{-3}
10^{-4}
10^{-5}
$\frac{d^2N}{dPd\Omega}$ sr -1 (Bev/c) -1 int. -1
5.7°
0°
0
2
4
6
8
10
12
14
$P_{\bar{p}}$ (Bev/c)

FIGURE 8

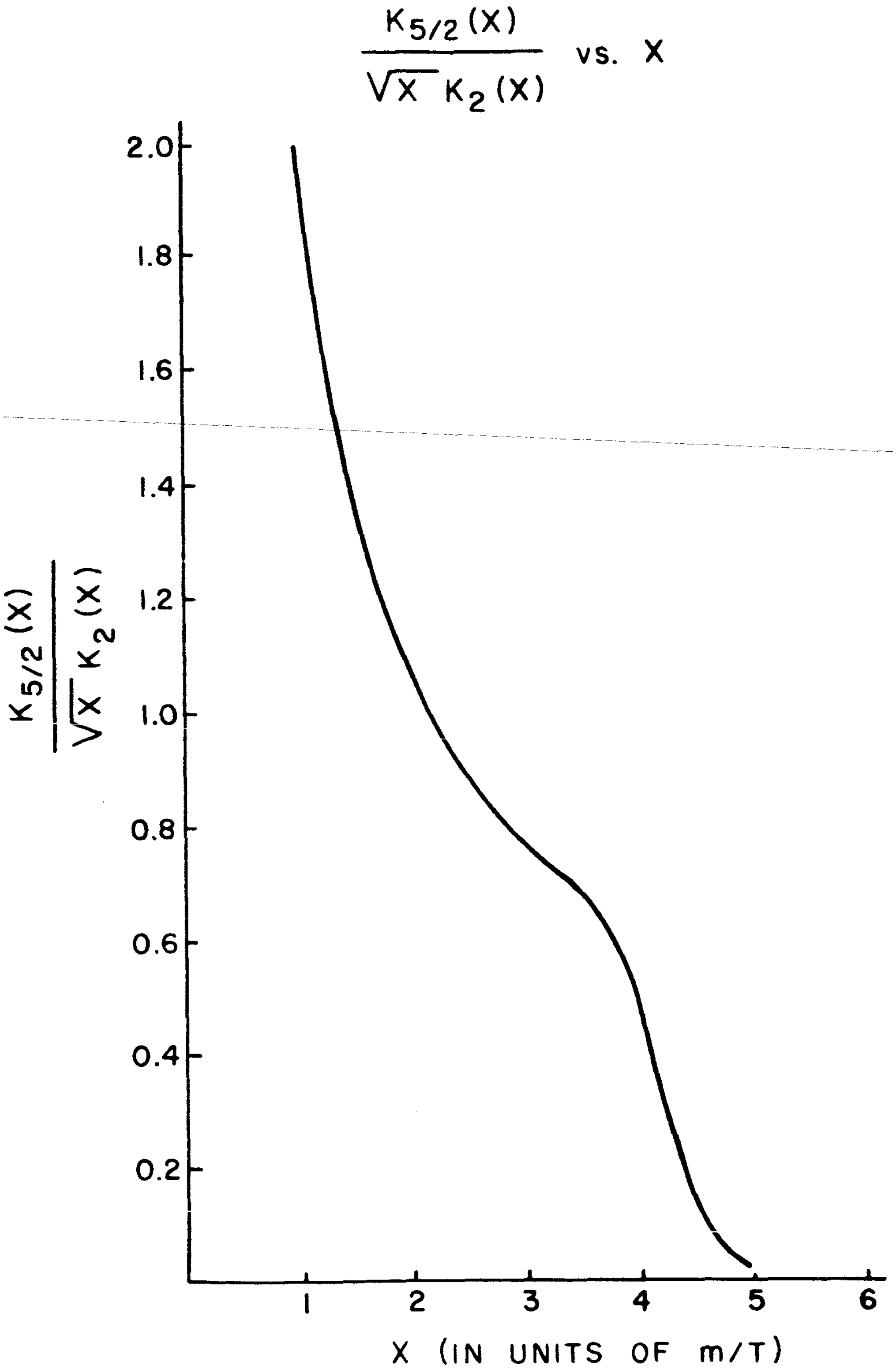
$\frac{K_{5/2}(X)}{\sqrt{X}\,K_2(X)}$ vs. X
2.0
1.8
1.6
1.4
1.2
1.0
0.8
0.6
0.4
0.2
$\frac{K_{5/2}(X)}{\sqrt{X}\,K_2(X)}$
1
2
3
4
5
6
X (IN UNITS OF m/T)

FIGURE 9